

2021

Numerical approach towards dynamic double shear testing of tendons using LS-DYNA

Saman Khaleghparast
University of Wollongong

Alex Remennikov
University of Wollongong

Naj Aziz
University of Wollongong

Follow this and additional works at: <https://ro.uow.edu.au/coal>

Recommended Citation

Saman Khaleghparast, Alex Remennikov, and Naj Aziz, Numerical approach towards dynamic double shear testing of tendons using LS-DYNA, in Naj Aziz and Bob Kininmonth (eds.), Proceedings of the 2021 Resource Operators Conference, Mining Engineering, University of Wollongong, 18-20 February 2019 <https://ro.uow.edu.au/coal/812>

Research Online is the open access institutional repository for the University of Wollongong. For further information contact the UOW Library: research-pubs@uow.edu.au

NUMERICAL APPROACH TOWARDS DYNAMIC DOUBLE SHEAR TESTING OF TENDONS USING LS-DYNA

Saman Khaleghparast¹, Alex Remennikov² and Naj Aziz³

ABSTRACT: Underground support systems using tendons has been one of the significant achievements in Civil and Mining engineering endeavors in facing the challenges of ground control. However, shear failure of rock bolts is a concern in underground excavations particularly with respect to seismic events. The understanding of the performance of rock bolts under dynamic loading condition requires a great deal of research. A series of tests were undertaken utilising a drop hammer mass of 592 kg dropped from a maximum height of 2 m onto grouted rock bolts encapsulated in concrete blocks in the double shear box to investigate the performance of rock bolts under dynamic shear load. Load cells, a displacement laser and high-speed camera were used to monitor the tests. Results from the data analyses are presented in the form of displacement, hammer mass drop velocity, force variation with time for all components involved in each test. A numerical simulation using ANSYS/LS-DYNA was used to simulate the behavior of 18 mm conventional rock bolts under high impact velocity loading conditions. The numerical simulation model was found to be in good agreement with the experimental results.

INTRODUCTION

Characterization of the strength of rock bolts and cable bolts for underground mining applications is generally based on tensile and shear strength. These two properties are determined by static testing, however in recent years, many tests have been reported with respect to the dynamically testing of rock bolts (Player, 2004, Plouffe, et al., 2008), The current thinking of ground reinforcement in underground mining has moved away from the emphasis being solely on ground support. The increased rate of mining development, production and mine operator safety are continuing to gain equal importance with ground support and its resilience in adverse mining environments. The prospect of ground seismicity and rock bursts requires special attention be focused to support infrastructure installation effectiveness, both in metal and coal mining. The Beaconsfield gold mine collapse, in Tasmania, triggered by seismic activity and pressure bursts at Austar coal mine, due to high levels of stress contribution caused by the presence of disturbed structural geology in the region with fault zones and shear zones as reported by Galvin and Hebblewhite (2016) are stark reminders of the challenges that mines are faced with in adverse conditions. This necessitates the need for credible research on ground support under these adverse conditions under both static and dynamic testing. The need for effective research on ground support credibility is of equal importance to the collapse of the ground due to gas outbursts, which are more common in coal mines worldwide and are well documented (<http://miningst.com/category/coal-mine-outburst/>). It is obvious that dynamic testing of tendons appears to focus on axial tensile testing and no reporting has been made on dynamic testing in shear. Tendon shear strength characteristics are important when shear deformation occurs across joints and shear zones, which are the weakest zones of the ground structure and that normally yield readily to rock burst or any other seismic activity. This paper describes the method of dynamic shear testing of tendons using double shear apparatus and compares the findings with the static method.

METHODOLOGY

The methodology used in this study will utilise testing of tendons by the double shear test rig, known as MK-I. The procedure of the testing was previously described in detail and it can be found from Khaleghparast, et al (2020).

¹ PhD candidate, Saman Khaleghparast. Email: sk329@uowmail.edu.au M: +61 (0) 423 812 516

² Professor, Alex Remennikov. Email: alexrem@uow.edu.au

³ Professor, Naj Aziz, Email: naj@uow.edu.au Tel: +61 2 42221 3449

The high-capacity impact machine

The drop hammer test method simulates a high energy impact load condition similar in amplitude and velocity to a rock burst event. Therefore, in this study, the drop hammer was employed to examine the impact and shear performance of conventional rock bolts and cable bolts. Figure 1 shows the schematic and general view of the drop hammer load impact rig. The core of the test rig is the free-fall hammer having a 592 Kg weight that can be dropped from a maximum height of 4.0 m, or equivalent to the drop velocity of up to 8.85 m/s. A 1200 kN dynamic load cell (Type Interface Model 1200) attached to the hammer measures the force applied to the medium at the time of the impact. The drop hammer test method simulates a high energy impact load condition similar in amplitude and velocity to a rock burst event. As the hammer falls, a laser gate triggers the load cell which allows data to be recorded by a data acquisition system. The collected data is transferred to a computer where the result can be analysed /processed. A high speed camera “Fastec trouble-shooter” was utilised to capture the high-energy impact between the drop hammer and the MK-I shear box with high accuracy. This allows an accurate analysis of the displacement of the central block during the shear load drop over the period of time. The shearing displacement of the central block was also monitored through utilising a laser placed underneath the central block. The MK-I set up box was seated on a U shape beam. The beam was placed between two base plates, which were anchored to the ground. The outer frames of the shear box were then clamped tightly to the base platform to avoid rotation of the blocks during drop loading impact.

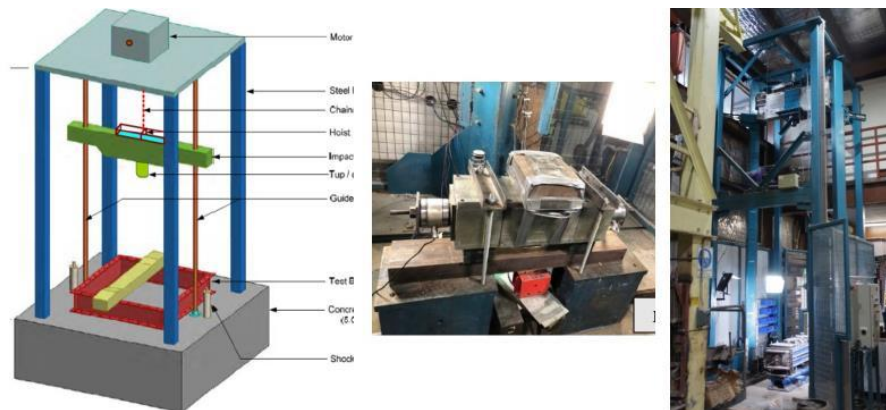


Figure 1: Drop hammer test and MK-I set up

To ensure that the load from the drop hammer is distributed evenly over the central block and also to prevent damaging to the box, a 30 mm thick plate was placed on top of the central block and covered with 3 mm thick plastic rubber. The potential height for each specimen was calculated based on the absorbed energy in the static test calculated from the area under the Load-displacement curve.

NUMERICAL MODELLING

The numerical analysis of the dynamic behaviour of rock bolts in a jointed rock mass, when subjected to extreme loading, can be studied using non-linear finite element software such as ABAQUS and LS-DYNA. In this study, ANSYS/LS-DYNA non-linear finite element software was considered. The advantage of using LS-DYNA is the efficient computational capability and the availability of a comprehensive material library. The current version of LS-DYNA contains more than 270 material models, of which 100 are constitutive models controlled by ten equations of state to cover a broad spectrum of materials (LSTC 2016, Bohara et al. 2019). LS-DYNA is the most widely used explicit analysis program, capable of simulating the response of material to short duration dynamic loading. Its many elements contact formulations, material models, and other controls can be used to simulate complex models with control over all the details of the problem. LS-DYNA can perform simulations of mechanisms involving joints and articulations subjected to impacts whether from drops or collisions. A three-dimensional (3D) FE model was generated using Strand7 software. Strand7 is a finite element analysis software that gives the user unparalleled functionality in a single application (Strand7 2010). Strand7 allows the user to have automatic mesh generation tools, working directly from the geometry.

It allows users to automatically generate 4-node and 10-node tetrahedral solid elements from 3D solid models. For this study, automatic surface mesh generation was used to create a high-quality FE mesh. The created mesh was composed of linear, quadratic triangular, and quadrilateral elements (3 node triangular elements and 4 node quadrilateral elements). After creating the geometry in Strand7, the file was exported to LS-PrePost for the dynamic analysis, shown in Figure 2. To represent the drop hammer, the 50 mm steel plate, the dynamic load cell as well as the tup, eight-node solid hexahedron elements with single-point integration were used. To reduce the computational time and make the simulations more efficient, one quarter of the entire body of the 3D model was considered due to the existing symmetry planes in the model.

Table 1: Results of static and dynamic tests carried out on 18 mm ribbed rock bolt

Test no.	Tendon type	Test properties					Test Results		Test Analysis			
		Pretension (kN)	Borehole Φ (mm)	Drop height (m)	Concrete strength (MPa)	Internal confinement	Static load (kN)	Dynamic load (kN)	70% static load (kN)	Effective friction (%)	Absorbed Energy (kJ)	
											Static	Dynamic
1	18 mm ribbed bolt	30	24	2	40	Yes	324	230	227	71	11.3	7.9
2	18 mm ribbed bolt	50	24	1.5	40	Yes	324	227	227	70	10.5	7.1
3	18 mm ribbed bolt	30	24	2	40	Yes	324	236	227	73	11.3	8.1
4	18 mm ribbed bolt	50	24	2	40	Yes	342	200	239.5	62	13.1	6.6
5	18 mm ribbed bolt	30	46	2	20	NO	331	160	232	50	13.5	4.7
6	18 mm ribbed bolt	50	24	2	60	NO	304	200	213	70	15.7	8.3
7	18 mm ribbed bolt	30	32	2	20	NO	331	190	232	60	13.5	11.1
8	18 mm ribbed bolt	50	32	2.5	60	NO	304	184	213	65	15.7	9.9

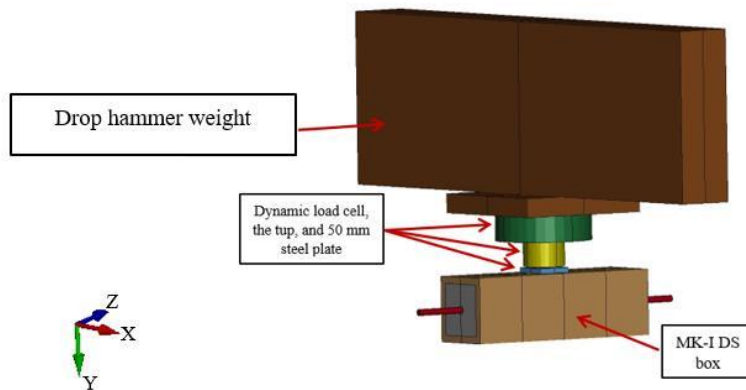


Figure 2: 3D model of MK-I DS box geometry as well as drop hammer compartments in LS-PrePost environment

The material models used in the FEM analysis was chosen as follows. The *Continuous_Surface_Cap_Model (CSCM, *MAT_159) was used for concrete and grout and the *Mat_Piecewise_Linear_Plasticity model (*MAT_024) was used for the rock bolt. The *Plastic_Kinematic model (*MAT_003) was used to simulate the steel confinement wrapped around the concrete blocks. The *RIGID model (*MAT_020) was used to simulate the drop hammer and the *ELASTIC model (*MAT_001) was used to simulate the load cell as well as the impact plate, respectively.

Overview of the CSCM model (*MAT_159)

CSCM model (*MAT_159) was originally proposed by Murray (2007). It is a developmental version of the concrete model that the developer has successfully employed and progressively enhanced since 1990 on defense contracts to analyse the dynamic loading of RC structures. This model has been implemented into the dynamic FE code, LS-DYNA, beginning with version 971. This model is in keyword format as *MAT_CSCM for CONTINUOUS_SURFACE_CAP_MODEL. Murray (2007) developed this material model to predict the dynamic behaviour, both elastic and plastic deformation or the failure of concrete material, which was used in roadside safety structures when involved in a collision with a motor vehicle. The user manual for LS-DYNA concrete material model 159 and Evaluation of LS-DYNA concrete material model 159 (FHWA-HRT-05-063) are the two documents that completely document this material model. This model includes initialisation routines that provide the user with the default input parameters for normal strength concrete. These initialisation routines set the required strengths, stiffness, hardening, softening, and rate effecting parameters as a function of concrete strength, maximum aggregate size, and the units.

Yield surface

The CSCM model consists of a smooth failure surface and uses damage mechanics to simulate strain softening and modulus degradation in both tensile and compression regimes as well as viscoelasticity for strain rate effects. It is a three-invariant extension of the *MAT_GEOLOGIC_CAP_Model (MAT_025). This model considers plastic flow and damage accumulations as a separate process based on the effective stress concept and the hypothesis of strain equivalence in continuum damage mechanics (CDM). The assumption for this model is that the shear stresses control the plastic flow, which may cause permanent deformation without causing degradation of elastic moduli, and the damage is assumed to result in the progressive degradation of the moduli. To model the plastic volume change, an elliptical cap surface was added to the model. This feature, besides concrete, is capable of modelling geo-materials including soils and rocks (Murray 2007). The model is a combination of a yield surface of a shear failure surface $F_f(I_1)$ and a cap surface $F_c(I_1, \kappa)$, with a continuous and smooth connection between the two as shown in Figure 3.

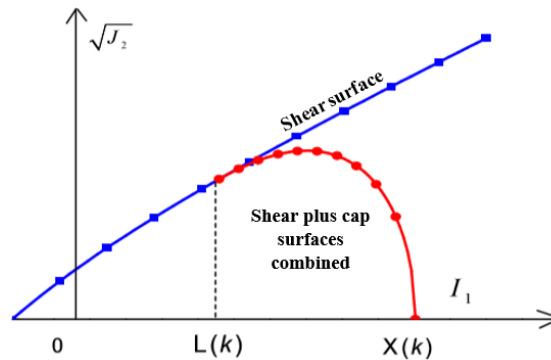


Figure 3: Graph of a multiplicative formulation of the shear and cap surfaces (adapted from (Murray 2007))

Damage formulation

Concrete shows strength reduction in the tensile and low-to-moderate compressive regimes. In this model, the softening or strength reduction is modeled via a damage formulation. Murray (2007) stated that without the damage formulation, the cap model predicts perfectly plastic behaviour for experimental simulation such as direct pull, unconfined compression, triaxial compression, and tri-axial extension, which is not realistic behaviour for concrete at lower confinement and in tension. The damage stress function can be written according to the effective stress concept in CDM:

$$\sigma = (1 - d)\bar{\sigma} \quad (1)$$

where the scalar damage variable d ($0 \leq d \leq 1$) grows from zero (undamaged material) to unity (completely damaged material with effective area reduced to zero). $(1 - d)$ is a reduction factor related

to the amount of damage at a material point. The accumulation of damage is based on two distinct formulations, which are known as brittle damage and ductile damage.

Overview of the Piecewise Linear Plasticity Model (MAT_024)

The PIECEWISE_LINEAR_PLASTICITY (*MAT_024) is an elasto-plastic material with an arbitrary stress-strain curve. In this model, a failure can be defined in two different ways including minimum step size or a plastic strain. This model is suitable and recommended by LSTC (2016) for solid elements. If the elastic strains of the material are finite before yielding, the material model treats the elastic strains using a hyper-elastic formulation. In this model the log interpolation keyword option is available, allowing the model to interpolate the strain rates in a table defined in LCSS with logarithmic interpolation. This model requires 28 parameters among which six parameters including density, young’s modulus, Poisson’s ratio, effective plastic true strain at failure, initial yield stress, and tangent modulus are required to simulate the model appropriately.

Stress-strain behaviour may be controlled by a bilinear stress-strain curve by defining the tangent modulus, shown as ETAN in the card. However, LSTC (2016) recommends calculating effective stress as a function of effective plastic strain. Figure 5 illustrates a curve of effective stress as a function of effective plastic strain.

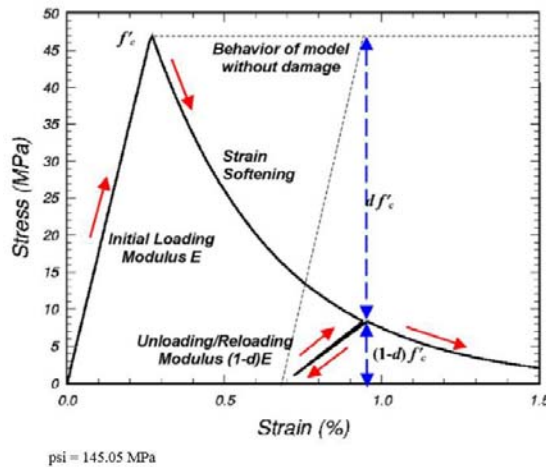


Figure 4: Strain softening and modulus reduction simulation using CSCM material model in LS-DYNA adapted from (Murray 2007)

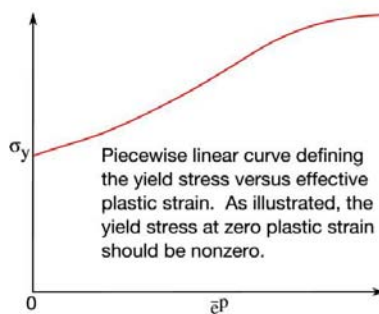


Figure 5: Effective stress as a function of the plastic strain curve for MAT_024 adopted from (LSTC 2016)

Accordingly, the true stress vs the true strain relationship was calculated for this model. It is recommended to input a smoothened stress-strain curve utilising a minimal number of points (LS-DYNA Support). The reason is that the experimental results always include some degree of error and tend to be somewhat noisy and erratic, which may create confusion within the model. Therefore, the smoother the stress-strain curve, the better the outcomes. Also, it is stated that the plastic strain in the defining curve should be the residual true strain after unloading elastically and true stress should be

used directly for stress values. Therefore, as an input, the curve shown in Figure 6 is defined as an input for the MAT24 model.

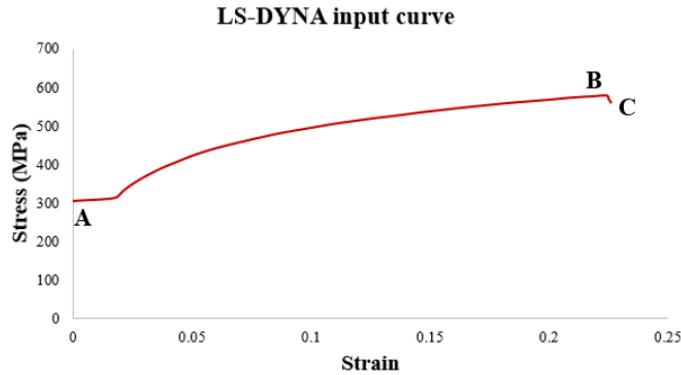


Figure 6: True stress versus plastic strain curve as an input in LS-DYNA

Mechanical response of MK-I in LS-DYNA

A 592 kg weight hammer was set to be dropped on the middle section of MK-I to create a dynamic double shear load in the system. In this regard, an initial impact velocity was set by choosing the drop hammer elements, measuring 6.3 m/s equal to 11.6 kJ of potential energy. Once the hammer dropped on the middle section, the whole section including the impactor, and the middle section including the rock bolt began to accelerate, travelling downward. The mechanical response of the whole system was found to be the same as what was expected from the laboratory experiments. In the model, once the impactor hits the box, the velocity of the impactor decreases whilst the velocity of the specimen increases.

Figure 7 illustrates the energy transformation from the kinetic energy of the impactor to the internal energy of the MK-I box predicted by the LS-DYNA. As it can be seen, once the impact occurred, the kinetic energy starts to decrease whilst the internal energy of the system begins to increase. The duration of this transformation of energy is 10 ms. Meaning that the kinetic energy of the impactor decreased to zero in 10 ms whilst the internal energy of the system increased significantly and reached 8.4 kJ. The hourglass energy is also presented in Figure 7, where it is calculated to be less than 7 % of the total energy. It was found that the amount of energy absorbed by the system is not the same as the total input energy, meaning some amount of energy was dissipated during the process of dynamic double shearing. Total energy was determined to be 11.6 kJ and only 8.4 kJ was absorbed by the system.

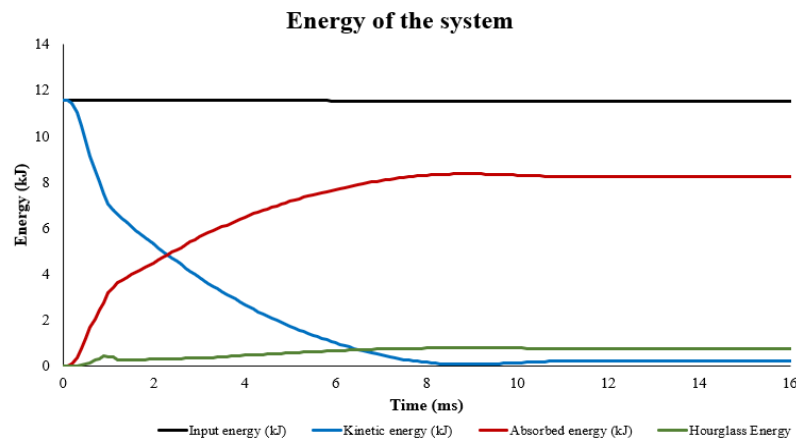


Figure 7: Total energy, kinetic energy versus absorbed energy, and hourglass energy in the system

To understand in detail what and how much energy is dissipated or how much energy is absorbed by the system a thorough investigation will be conducted on individual components of the system including the rock bolt, grout, concrete blocks, and steel casing confinement in the following.

Table 2 represents the calculated velocity and energy absorption of the MK-I apparatus in experimental and numerical tests.

Table 2: Velocity and energy absorption by MK-I in numerical and experimental results

Experimental results				Numerical results				
Test No.	Velocity (m/s)	Absorbed energy (kJ)	Absorbed energy / total input energy (%)	Part	Velocity (m/s)	Absorbed energy (kJ)	Part energy/total absorbed energy (%)	
2	4.38	7.1	68	MK-I	Impact plate	5.75	0.15	1.3
					Mid steel confinement	6.35	2.0	17
3	5.23	8.1	72		Mid concrete	6.20	1.5	13
					Grout	3.2	0.4	3.5
4	4.75	6.6	60		Rock bolt	3.2	3.0	26
					Side steel confinement	0	0.3	2.6
Average	4.78	7.3	67%		Side concrete	0	1.05	9
					Total	4.94	8.4	72%

Looking at the numerical results, the energy as well as the velocity of each element measured and recorded in Table 2. The velocity of concrete and steel confinement is much the same and measured as 6.20 and 6.35 m/s respectively. On the other hand, the velocity of the rock bolt and grout is recorded as being the same at 3.2 m/s. However, the amount of energy that the rock bolt can absorb in comparison with grout is significantly different. The contribution of the rock bolt in absorbing energy is 26 % of the internal energy in the system, whilst grout only absorbed 3.5 % of the internal energy. It is understandable that the rock bolt plays a pivotal role in the system and it can simply define the stiffness of the system. The role of grout, however in the dynamic double shear testing is not as important as it is in static loading conditions. In low strain loading conditions, the grout acts as a strong bonding element between concrete and the rock bolt. However, since the grout has a high compressive strength of almost 65 MPa for this study, it can absorb less energy, because of its brittle nature. Therefore, it is understandable that as soon as energy travels through the material, the grout will crust quickly. The steel confinement and concrete block in the middle section, on the other hand, absorb a great deal of energy from the system, 20 and 13 %, respectively.

Comparing the results from an experiment with a numerical model based on energy absorption can confirm that the mechanical response of the MK-I in numerical results is in good agreement with the experimental results. In both situations, almost 70 % of the total input energy is absorbed by the system. Furthermore, the velocity of the system is in good agreement with the calculated velocity of the system driven from experiments. It can be observed that the average calculated velocity from the tests of the MK-I is 4.78 m/s and the velocity of the system in the numerical model is measured as 4.94 m/s. This proves that the system's response in the numerical model is very similar to the response of the physical system.

Figure 8 demonstrates the impact load versus time histories of the double shear test in the experiment and numerical simulation.

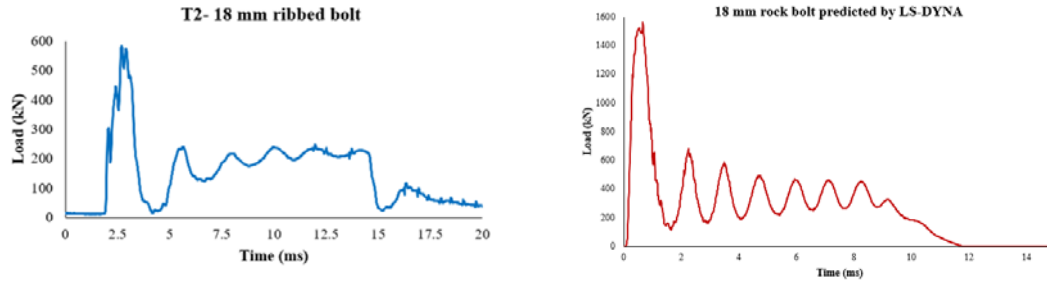


Figure 8: Impact load versus time in the experimental results as well as numerical simulation

It is thus clear that the impact load versus time from the numerical modeling is in good agreement with experimental results. The impact load versus time has three-stages of loading. The first stage is the inertia effect which is quite high when compared with the experiment. The second stage is when the model is moving downward along with the impactor which creates a low-frequency oscillation in the load-time curve. Nevertheless, the impact load in the numerical simulation is almost doubled as it is in the experiment. This could be due to the usage of a thick rubber pad between the impactor and impact plate in the real experiments. The rubber apparently could reduce the impact load by reducing the effect of inertial force at the moment of impact. However, a great deal of effort has been put in to include a rubber pad in the model to examine the response of the system. However, designing a 3 to 5 mm thick rubber pad as a hyper-elastic material in such a huge energy impact was concluded to be impossible, due to the inability of the software to simulate the situation. Therefore, the effect of the rubber pad between the impactor and impact plate was neglected and the impact was performed directly on the steel enclosure. Still, by excluding the rubber, the model was recognised as a reliable tool to study the response of rock bolt under impact load.

The development of energy along the 18 mm Jennmar rock bolt

When a bar is loaded laterally, it is deformed into a curve, and the resulting stresses and strains are directly related to the deflected curve, which is affected by the surrounding materials (Jalalifar, 2006). Figure 9 demonstrates the stress development in the rock bolt at joint faces at the point of impact. Once the load is exerted on the specimen at $t=0.6$ ms, a part of the energy is immediately transferred to the rock bolt at the joint faces. The figure illustrates half of the model.

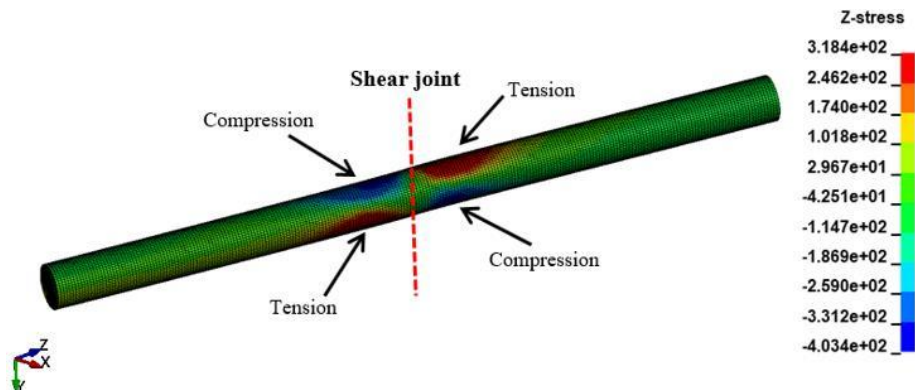


Figure 9: General view of axial stress development in half of the rock bolt at $t=0.6$ ms

As can be seen from the graph, the developed stress at the time of impact on the rock bolt at $t= 0.6$ ms is higher than the yield strength of the rock bolt. The yield stress of the rock bolt was measured as 306 MPa and the maximum stress imposed on the rock bolt in the tension and compression zone is 318 and 403 MPa, respectively. The tension was shown by positive values and compression was marked by negative values. The high amount of stress at the time of impact can be interpreted in a

way that the rock bolt starts deforming plastically, immediately after the impact. This prevents the development of axial stress in the rock bolt as a significant amount of energy in the form of concentrated energy is developed in the vicinity of the shear joints. The concentrated energy in the vicinity of the joint gradually increases, starting with plastic deformation and ends with a rupture at 10 ms. From the theory, it is known that the shear stress in the vicinity of joints is the highest and reduces from the shear face towards the bolt end. On the other hand, the bending moment (hinge point) in the shear face is zero. The maximum effective Von Mises stress is 872 MPa which can create 224 kN of shear load at 8 ms with a shear displacement of 44 mm, as is shown in Figure 10.

The shear load is developed at the shear zones under the initial impact velocity of 6.3 m/s. The built-up shear force can rupture the 18 mm Jenmar ribbed rock bolt as the load exceeds its ultimate tensile strength. Table 3 shows the numerical and experimental results under impact loading conditions. The average shear load from four experimental results was measured as 223 kN and the deflection of the bolt was determined as 42 mm. From the numerical results, the peak shear load was measured as 224 kN with a shear displacement of 44 mm.

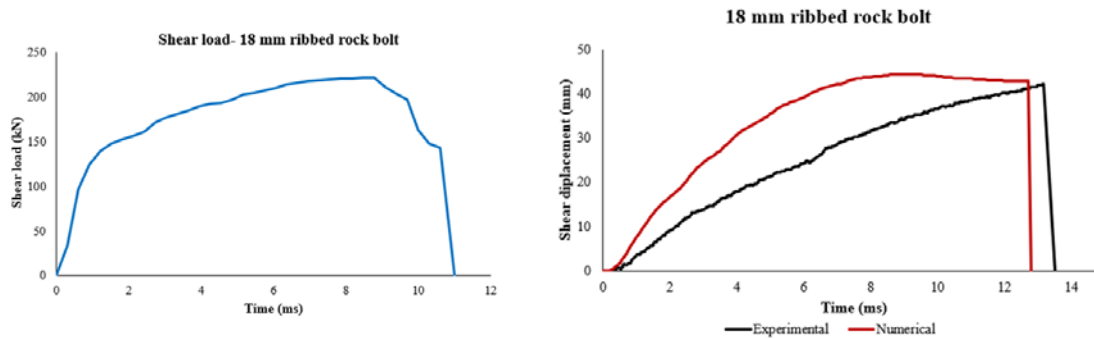


Figure 10: Dynamic shear load vs time as well as dynamic shear displacement vs time predicted by LS-DYNA

Table 3: Numerical and experimental results for fully grouted 18 mm rock bolt

Sample properties			Experimental results			Numerical results	
Test No	Borehole \varnothing (mm)	Concrete strength (MPa)	Static load (kN)	Dynamic load (kN)	Displacement (mm)	Dynamic load (kN)	Displacement (mm)
1	24	40	324	230	-	224	44
2	24	40	324	227	40	224	44
3	24	40	324	236	42	224	44
4	24	40	342	200	45	224	44
Average				223	42	224	44

As can be seen, both the shear load and the deformation captured from the numerical results are in relatively good agreement with the experimental results. Therefore, it is safe to say that the numerical model can predict the shear load as well as shear displacement under impact loading conditions.

Friction effect

Calculation of the frictional energy was undertaken through activation of FRCENG to 1.0 in the menu of control_contact. By activating this option, the frictional energy between all elements that have been defined by the Contact algorithms is calculated. The results are recorded by activating an option SLEOUT. On the other hand, the total sliding energy is also calculated through the GLSTAT command. Some 2.35 kJ of the total energy was wasted as sliding energy to overcome the friction between each component, meaning that 20% of the total energy is wasted through friction between each part. These contacts are between confinement and concrete, grout and concrete, grout and rock bolt, middle confinement and side confinement, and middle concrete to side concrete. Figure 11 shows the energy absorption between each part due to friction.

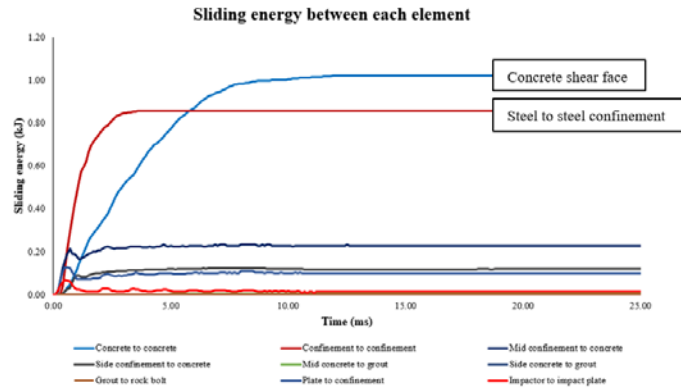


Figure 11: Dissipation of energy to overcome the friction between each element

As can be seen from the graph, 80 % of the wasted energy is lost through overcoming the friction between the shear faces, which is sliding between mid and side confinement as well as concrete. The frictional energy in the shear joint was recorded as 1.9 kJ which is almost 20 % of the input energy.

Figure 12 shows the ratio of energy dissipated due to the erosion effect. Eroded energy is the energy associated with deleted elements (internal energy) and deleted nodes (kinetic energy) due to a negative influence on the calculation. Approximately 8 % of the energy dissipated in the system is due to erosion. This 8 % of energy loss was previously interpreted as energy loss due to vibration, heat, noise, and cracking in concrete blocks, without quantifying this amount.

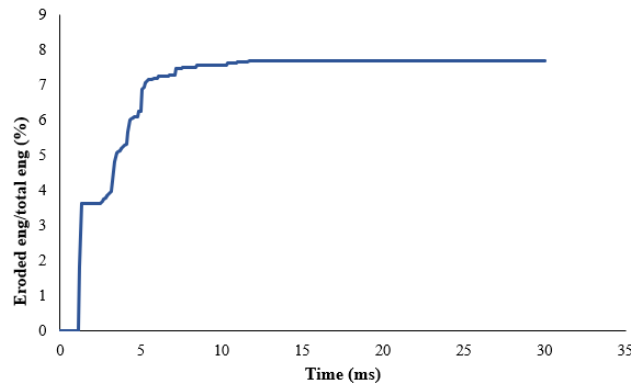


Figure 12: Energy dissipation in the system due to erosion

CONCLUSIONS

Dynamic response of conventional 18 mm ribbed rock bolt was investigated numerically using LS-DYNA under impact loading conditions. The mechanical response of the MK-I double shear box under high-velocity impact loads was assessed using 40 MPa concrete blocks. It was found that the model could predict the dynamic shear load as well as dynamic shear displacement of the 18 mm rock bolt under impact load. The following conclusions can be drawn:

- The impact load in the numerical model was almost double that of the experimental results. This was interpreted as the effect of using a 3 mm rubber pad between the impactor and impact plate during the impact experiments.
- The contribution of the rock bolt in absorbing energy was the highest among each component of the specimen, absorbing 26 % of the internal energy before steel casing confinement and concrete with 20 and 13 %, respectively. The rock bolt can define the stiffness of the MK-I double shear box in dynamic double shear testing.

- 70 % of the total input energy is absorbed by the MK-I double shear apparatus. This percentage was in good agreement with the experimental results.
- Only 20 % of the total input energy went to overcome the friction between joints, which was the friction between the steel confinement and concrete faces. Furthermore, only 8 % of the energy was wasted due to the effect of erosion activated in the numerical model.

REFERENCES

- Aziz, N, Craig, P, Mirzaghobanali, A, Rasekh, H, Nemcik, J and Li, X, 2015b. Behaviour of cable bolts in shear; experimental study and mathematical modelling. *Coal Operators' Conference*, pp. 146-159 (Wollongong, University of Wollongong). <http://ro.uow.edu.au/coal/559/>
- Aziz, N, Mirza, A, Nemick, J, Li, X, Rasekh, H and Wang, G, 2016a. Load Transfer Characteristics of plain and spiral cable bolts tested in new non-rotating pull testing apparatus, *Coal Operators' Conference*, pp. 32-39 (Wollongong, University of Wollongong). <http://ro.uow.edu.au/coal/591/>
- Aziz, N, Mirza, A, Nemcik, J, Rasekh, H and Li, X, 2016b. A Follow up to Study the Behaviour of Cable Bolts in Shear: Experimental Study and Mathematical Modelling, *Coal Operators' Conference*, pp. 24-31 (Wollongong, University of Wollongong). <http://ro.uow.edu.au/coal/590/>
- Bohara, R P, Tanapornraweekit, G, and Tangtermsirikul, S, 2019. Investigation of concrete material models for analysis of seismic behavior of reinforced concrete under reversed cyclic load. *Songklanakirin Journal of Science and Technology*.
- British Standard BS7861-1, 2009. Strata reinforcement support systems components used in coal mines – Part 2: Specification for flexible systems for roof reinforcement, 48p.
- Khaleghparast S, Anzanpour S, Aziz N, Remennikov A, Mirzaghobanali A, 2020. Static and dynamic testing of tendons. *Coal Operators' Conference*, pp. 146-154 (Wollongong, University of Wollongong). (<https://ro.uow.edu.au/cgi/viewcontent.cgi?article=2430&context=coal>).
- LSTC (2016). LS-DYNA Keyword User's Manual Version 971, Livermore Software Technology Corporation.
- Murray, Y. D., 2007. User's manual for LS-DYNA concrete material model 159, United States. Federal Highway Administration. Office of Research.
- Plouffe m, Anderson T, Judge K, 2008. Rock bolts testing under dynamic conditions at Cenmet-MMSL, in proc 6th international Symposium on ground support in mining and civil construction, TR Stacey and D F Malan(eds) 30th March -3rd April 2008, Cape town, South Africa< the south African Institute of Min and Met], Johannesburg, pp 581 -395.
- Player, J P , Villaescusa, E and Thompson, A G., 2004, Dynamic testing of rock reinforcement using the momentum transfer concept, Ground support in mining and underground construction, *Proceedings of the fifth international Symposium on ground support*, 28-30 September, Perth, pp 327-339 (Ed: Ernesto Villaescusa and Yves Potvin).
- Stillborg, B, 1984. Experimental investigation of steel cables for rock reinforcement in hard rock. PhD Thesis, Lulea University, Sweden.
- Strand 7, 2010. Introduction to the Strand7 finite element analysis system.
- Villaescusa E, Thompson, A and Player J R, 2005. Dynamic testing of ground support systems, Phase I, MERIWA project No M3492, 10s9 p.